Flexible Joints - Test Bench

Dehaeze Thomas

April 30, 2024

Contents

At both ends of the nano-hexapod struts, a flexible joint is used. Ideally, these flexible joints would behave as perfect spherical joints, that is to say no bending and torsional stiffness, infinite shear and axial stiffness, unlimited bending and torsional stroke, no friction, and no backlash.

Deviations from these ideal properties will impact the dynamics of the Nano-Hexapod and could limit the attainable performance. During the detailed design phase, specifications in terms of stiffness and stroke were determined and are summarized in Table 1.

	Specification	**FEM**
Axial Stiffness	$> 100\,N/\mu m$	94
Shear Stiffness	$> 1\,N/\mu m$	13
Bending Stiffness	$< 100\,Nm/\text{rad}$	5
Torsion Stiffness	$< 500\,Nm/\text{rad}$	260
Bending Stroke	$> 1\,\text{mrad}$	24.5

Table 1: Specifications for the flexible joints and estimated characteristics from the Finite Element Model

After optimization using a finite element model, the geometry shown in Figure 1 has been obtained and the corresponding flexible joint characteristics are summarized in Table 1. This flexible joint is a monolithic piece of stainless steel[1] manufactured using wire electrical discharge machining. It serves several functions, as shown in Figure 1a, such as:

- Rigid interfacing with the nano-hexapod plates (yellow surfaces)
- Rigid interfacing with the amplified piezoelectric actuator (blue surface)
- Allow two rotations between the "yellow" and the "blue" interfaces. The rotation axes are represented by the dashed lines that intersect

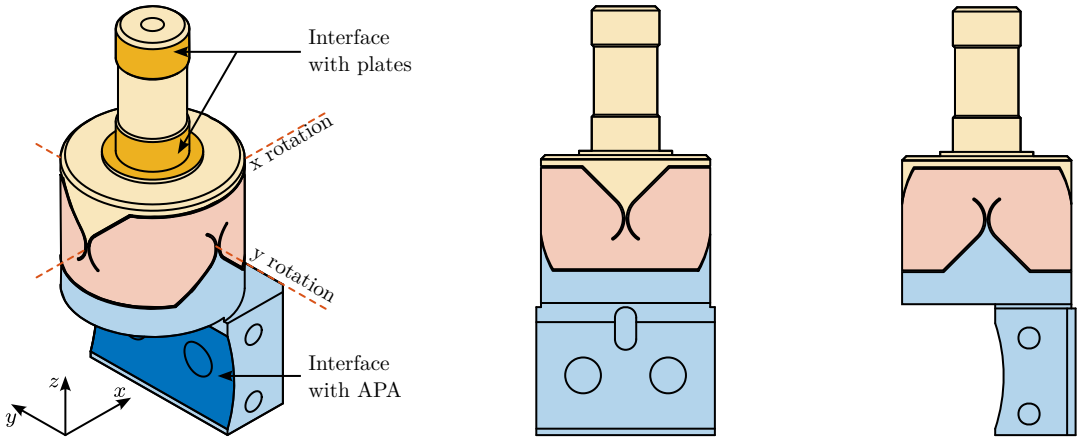

(a) ISO view **(b)** YZ plane **(c)** XZ plane

Figure 1: Geometry of the optimized flexible joints

Sixteen flexible joints have been ordered (shown in Figure 2a) such that some selection can be made for the twelve that will be used on the nano-hexapod.

[1]The alloy used is called *F16PH*, also refereed as "1.4542"

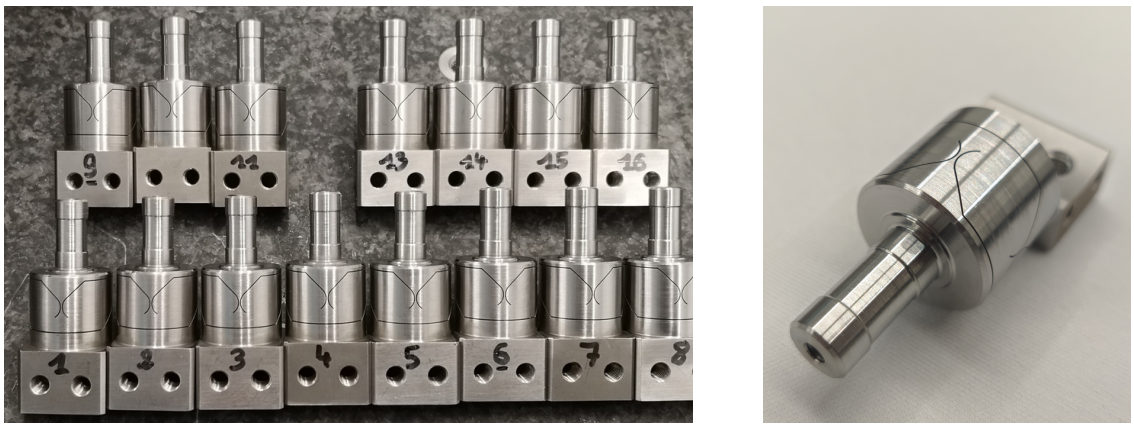

(a) 15 of the 16 received flexible joints

(b) Zoom on one flexible joint

Figure 2: Pictures of the received 16 flexible joints

In this document, the received flexible joints are characterized to ensure that they fulfill the requirements and such that they can well be modeled.

First, the flexible joints are visually inspected, and the minimum gaps (responsible for most of the joint compliance) are measured (Section 1). Then, a test bench was developed to measure the bending stiffness of the flexible joints. The development of this test bench is presented in Section 2, including a noise budget and some requirements in terms of instrumentation. The test bench is then used to measure the bending stiffnesses of all the flexible joints. Results are shown in Section 3

1 Dimensional Measurements

1.1 Measurement Bench

Two dimensions are critical for the bending stiffness of the flexible joints. These dimensions can be measured using a profilometer. The dimensions of the flexible joint in the Y-Z plane will contribute to the X-bending stiffness, whereas the dimensions in the X-Z plane will contribute to the Y-bending stiffness.

The setup used to measure the dimensions of the "X" flexible beam is shown in Figure 1.1a. What is typically observed is shown in Figure 1.1b. It is then possible to estimate the dimension of the flexible beam with an accuracy of $\approx 5\,\mu m$,

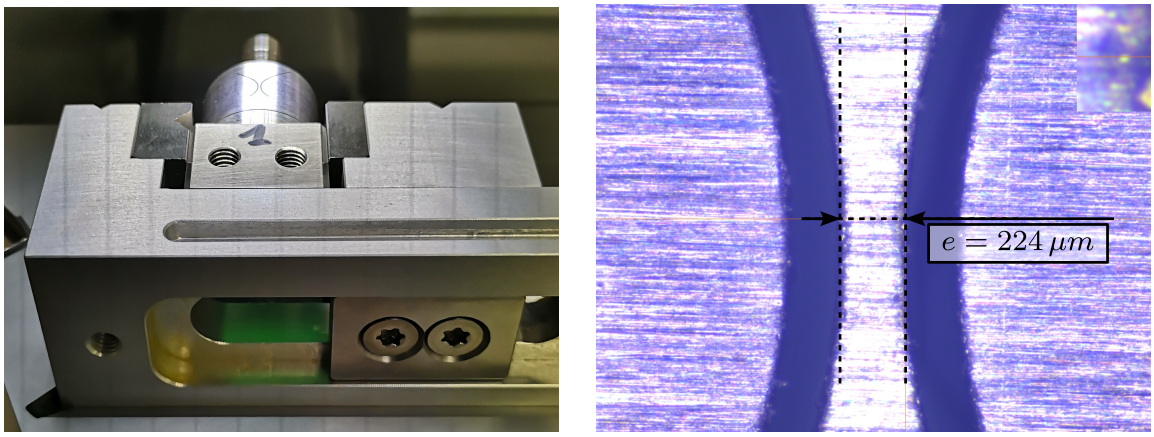

(a) Flexible joint fixed on the profilometer

(b) Picture of the gap

Figure 1.1: Setup to measure the dimension of the flexible beam corresponding to the X-bending stiffness. The flexible joint is fixed to the profilometer (a) and a image is obtained with which the gap can be estimated (b)

1.2 Measurement Results

The specified flexible beam thickness (gap) is $250\,\mu m$. Four gaps are measured for each flexible joint (2 in the x direction and 2 in the y direction). The "beam thickness" is then estimated as the mean between the gaps measured on opposite sides.

A histogram of the measured beam thicknesses is shown in Figure 1.2. The measured thickness is less than the specified value of $250\,\mu m$, but this optical method may not be very accurate because the estimated gap can depend on the lighting of the part and of its proper alignment.

However, what is more important than the true value of the thickness is the consistency between all flexible joints.

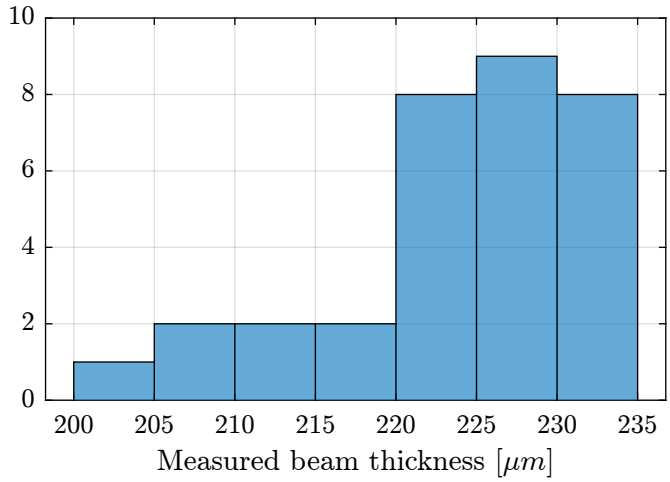

Figure 1.2: Histogram for the (16x2) measured beams' thicknesses

1.3 Bad flexible joints

Using this profilometer allowed to detect flexible joints with manufacturing defects such as non-symmetrical shapes (see Figure 1.3a) or flexible joints with machining chips stuck in the gap (see Figure 1.3b).

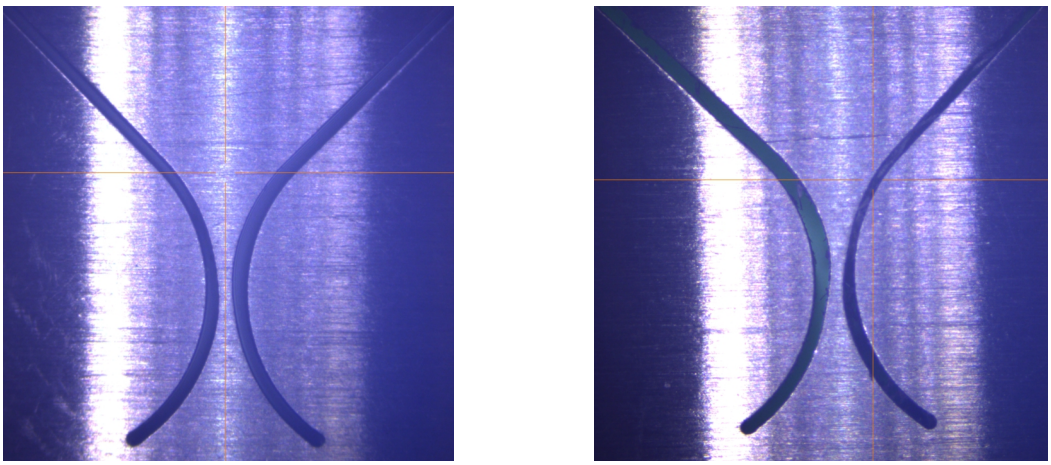

(a) Non-Symmetrical shape

(b) "Chips" stuck in the air gap

Figure 1.3: Example of two flexible joints that were considered unsatisfactory after visual inspection

2 Compliance Measurement Test Bench

The most important characteristic of the flexible joint to be measured is its bending stiffness $k_{R_x} \approx k_{R_y}$.

To estimate the bending stiffness, the basic idea is to apply a torque T_x to the flexible joints and to measure its angular deflection θ_x. The bending stiffness can then be computed from equation (2.1).

$$\boxed{k_{R_x} = \frac{T_x}{\theta_x}, \quad k_{R_y} = \frac{T_y}{\theta_y}} \tag{2.1}$$

2.1 Measurement principle

Torque and Rotation measurement To apply torque T_y between the two mobile parts of the flexible joint, a known "linear" force F_x can be applied instead at a certain distance h with respect to the rotation point. In this case, the equivalent applied torque can be estimated from equation (2.2). Note that the application point of the force should be sufficiently far from the rotation axis such that the resulting bending motion is much larger than the displacement due to shear. Such effects are studied in Section 2.2.

$$T_y = hF_x, \quad T_x = hF_y \tag{2.2}$$

Similarly, instead of directly measuring the bending motion θ_y of the flexible joint, its linear motion d_x at a certain distance h from the rotation points is measured. The equivalent rotation is estimated from (2.3).

$$\theta_y = \tan^{-1}\left(\frac{d_x}{h}\right) \approx \frac{d_x}{h}, \quad \theta_x = \tan^{-1}\left(\frac{d_y}{h}\right) \approx \frac{d_y}{h} \tag{2.3}$$

Then, the bending stiffness can be estimated from (2.4).

$$k_{R_x} = \frac{T_x}{\theta_x} = \frac{hF_y}{\tan^{-1}\left(\frac{d_y}{h}\right)} \approx h^2\frac{F_y}{d_y} \tag{2.4a}$$

$$k_{R_y} = \frac{T_y}{\theta_y} = \frac{hF_x}{\tan^{-1}\left(\frac{d_x}{h}\right)} \approx h^2\frac{F_x}{d_x} \tag{2.4b}$$

The working principle of the measurement bench is schematically shown in Figure 2.1. One part of the flexible joint is fixed to a rigid frame while a (known) force F_x is applied to the other side of the flexible joint. The deflection of the joint d_x is measured using a displacement sensor.

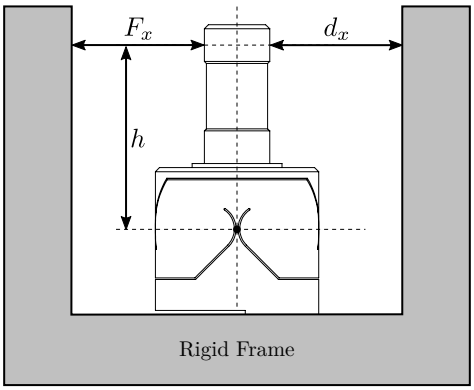

Figure 2.1: Working principle of the test bench used to estimate the bending stiffness k_{R_y} of the flexible joints by measuring F_x, d_x and h

Required external applied force The bending stiffness is foreseen to be $k_{R_y} \approx k_{R_x} \approx 5\,\frac{Nm}{rad}$ and its stroke $\theta_{y,\max} \approx \theta_{x,\max} \approx 25\,mrad$. The height between the flexible point (center of the joint) and the point where external forces are applied is $h = 22.5\,mm$ (see Figure 2.1).

The bending θ_y of the flexible joint due to the force F_x is given by equation (2.5).

$$\theta_y = \frac{T_y}{k_{R_y}} = \frac{F_x h}{k_{R_y}} \tag{2.5}$$

Therefore, the force that must be applied to test the full range of the flexible joints is given by equation (2.6). The measurement range of the force sensor should then be higher than $5.5\,N$.

$$F_{x,\max} = \frac{k_{R_y}\theta_{y,\max}}{h} \approx 5.5\,N \tag{2.6}$$

Required actuator stroke and sensors range The flexible joint is designed to allow a bending motion of $\pm 25\,mrad$. The corresponding stroke at the location of the force sensor is given by (2.7). To test the full range of the flexible joint, the means of applying a force (explained in the next section) should allow a motion of at least $0.5\,mm$. Similarly, the measurement range of the displacement sensor should also be higher than $0.5\,mm$.

$$d_{x,\max} = h\tan(R_{x,\max}) \approx 0.5\,mm \tag{2.7}$$

Force and Displacement measurements To determine the applied force, a load cell will be used in series with the mechanism that applied the force. The measured deflection of the flexible joint will be indirectly estimated from the displacement of the force sensor itself (see Section 2.3). Indirectly measuring the deflection of the flexible joint induces some errors because of the limited stiffness between

the force sensor and the displacement sensor. Such an effect will be estimated in the error budget (Section 2.2)

2.2 Error budget

To estimate the accuracy of the measured bending stiffness that can be obtained using this measurement principle, an error budget is performed.

Based on equation (2.4), several errors can affect the accuracy of the measured bending stiffness:

- Errors in the measured torque M_x, M_y: this is mainly due to inaccuracies in the load cell and of the height estimation h
- Errors in the measured bending motion of the flexible joints θ_x, θ_y: errors from limited shear stiffness, from the deflection of the load cell itself, and inaccuracy of the height estimation h

If only the bending stiffness is considered, the induced displacement is described by (2.8).

$$d_{x,b} = h \tan(\theta_y) = h \tan\left(\frac{F_x \cdot h}{k_{R_y}}\right) \tag{2.8}$$

Effect of Shear The applied force F_x will induce some shear $d_{x,s}$ which is described by (2.9) with k_s the shear stiffness of the flexible joint.

$$d_{x,s} = \frac{F_x}{k_s} \tag{2.9}$$

The measured displacement d_x is affected shear, as shown in equation (2.10).

$$d_x = d_{x,b} + d_{x,s} = h \tan\left(\frac{F_x \cdot h}{k_{R_y}}\right) + \frac{F_x}{k_s} \approx F_x \left(\frac{h^2}{k_{R_y}} + \frac{1}{k_s}\right) \tag{2.10}$$

The estimated bending stiffness k_{est} then depends on the shear stiffness (2.11).

$$k_{R_y,\text{est}} = h^2 \frac{F_x}{d_x} \approx k_{R_y} \frac{1}{1 + \frac{k_{R_y}}{k_s h^2}} \approx k_{R_y} \Big(1 - \underbrace{\frac{k_{R_y}}{k_s h^2}}_{\epsilon_s}\Big) \tag{2.11}$$

With an estimated shear stiffness $k_s = 13\, N/\mu m$ from the finite element model and an height $h = 25\, mm$, the estimation errors of the bending stiffness due to shear is $\epsilon_s < 0.1\,\%$

Effect of load cell limited stiffness As explained in the previous section, because the measurement of the flexible joint deflection is indirectly performed with the encoder, errors will be made if the load cell experiences some compression.

Suppose the load cell has an internal stiffness k_f, the same reasoning that was made for the effect of shear can be applied here. The estimation error of the bending stiffness due to the limited stiffness of the load cell is then described by (2.12).

$$k_{R_y,\text{est}} = h^2 \frac{F_x}{d_x} \approx k_{R_y} \frac{1}{1 + \frac{k_{R_y}}{k_F h^2}} \approx k_{R_y} \Big(1 - \underbrace{\frac{k_{R_y}}{k_F h^2}}_{\epsilon_f}\Big) \tag{2.12}$$

With an estimated load cell stiffness of $k_f \approx 1\, N/\mu m$ (from the documentation), the errors due to the load cell limited stiffness is around $\epsilon_f = 1\,\%$.

Estimation error due to height estimation error Now consider an error δh in the estimation of the height h as described by (2.13).

$$h_{\text{est}} = h + \delta h \tag{2.13}$$

The computed bending stiffness will be (2.14).

$$k_{R_y,\text{est}} \approx h_{\text{est}}^2 \frac{F_x}{d_x} \approx k_{R_y} \Big(1 + \underbrace{2\frac{\delta h}{h} + \frac{\delta h^2}{h^2}}_{\epsilon_h}\Big) \tag{2.14}$$

The height estimation is foreseen to be accurate to within $|\delta h| < 0.4\, mm$ which corresponds to a stiffness error $\epsilon_h < 3.5\,\%$.

Estimation error due to force and displacement sensors accuracy An optical encoder is used to measure the displacement (see Section 2.3) whose maximum non-linearity is $40\, nm$. As the measured displacement is foreseen to be $0.5\, mm$, the error ϵ_d due to the encoder non-linearity is negligible $\epsilon_d < 0.01\,\%$.

The accuracy of the load cell is specified at $1\,\%$ and therefore, estimation errors of the bending stiffness due to the limited load cell accuracy should be $\epsilon_F < 1\,\%$

Conclusion The different sources of errors are summarized in Table 2.1. The most important source of error is the estimation error of the distance between the flexible joint rotation axis and its contact with the force sensor. An overall accuracy of $\approx 5\,\%$ can be expected with this measurement bench, which should be sufficient for an estimation of the bending stiffness of the flexible joints.

Effect	Error
Shear effect	$\epsilon_s < 0.1\,\%$
Load cell compliance	$\epsilon_f = 1\,\%$
Height error	$\epsilon_h < 3.5\,\%$
Displacement sensor	$\epsilon_d < 0.01\,\%$
Force sensor	$\epsilon_F < 1\,\%$

Table 2.1: Summary of the error budget for estimating the bending stiffness

2.3 Mechanical Design

As explained in Section 2.1, the flexible joint's bending stiffness is estimated by applying a known force to the flexible joint's tip and by measuring its deflection at the same point.

The force is applied using a load cell[1] such that the applied force to the flexible joint's tip is directly measured. To control the height and direction of the applied force, a cylinder cut in half is fixed at the tip of the force sensor (pink element in Figure 2.2b) that initially had a flat surface. Doing so, the contact between the flexible joint cylindrical tip and the force sensor is a point (intersection of two cylinders) at a precise height, and the force is applied in a known direction. To translate the load cell at a constant height, it is fixed to a translation stage[2] which is moved by hand.

Instead of measuring the displacement directly at the tip of the flexible joint (with a probe or an interferometer for instance), the displacement of the load cell itself is measured. To do so, an encoder[3] is used, which measures the motion of a ruler. This ruler is fixed to the translation stage in line (i.e. at the same height) with the application point to reduce Abbe errors (see Figure 2.2a).

The flexible joint can be rotated by 90^o in order to measure the bending stiffness in the two directions. The obtained CAD design of the measurement bench is shown in Figure 2.2a while a zoom on the flexible joint with the associated important quantities is shown in Figure 2.2b.

[1] The load cell is FC22 from TE Connectivity. The measurement range is $50\,N$. The specified accuracy is $1\,\%$ of the full range

[2] V-408 PIMag® linear stage is used. Crossed rollers are used to guide the motion.

[3] Resolute™ encoder with $1\,nm$ resolution and $\pm 40\,nm$ maximum non-linearity

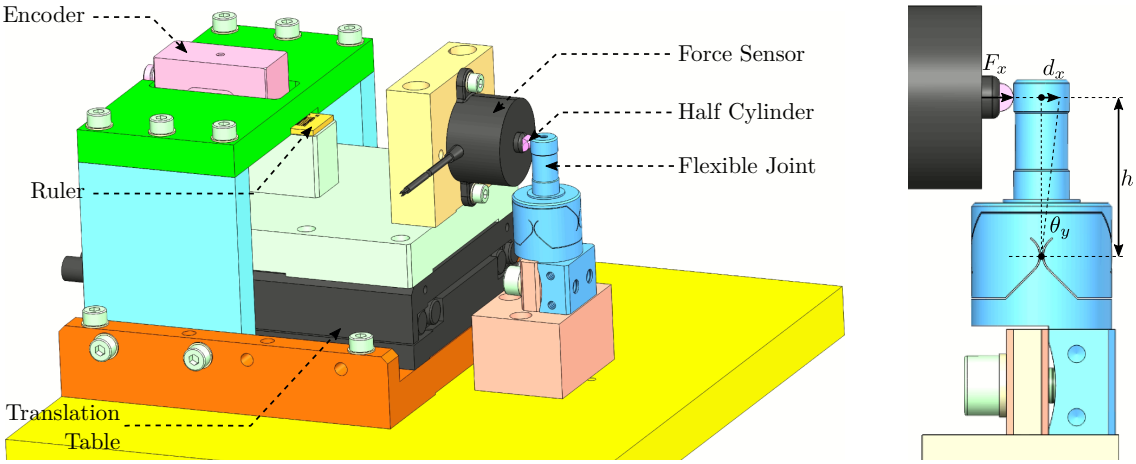

(a) Schematic of the test bench to measure the bending stiffness of the flexible joints **(b)** Zoom

Figure 2.2: CAD view of the test bench developed to measure the bending stiffness of the flexible joints. Different parts are shown in (a) while a zoom on the flexible joint is shown in (b)

3 Bending Stiffness Measurement

A picture of the bench used to measure the X-bending stiffness of the flexible joints is shown in Figure 3.1a. A closer view of the force sensor tip is shown in Figure 3.1b.

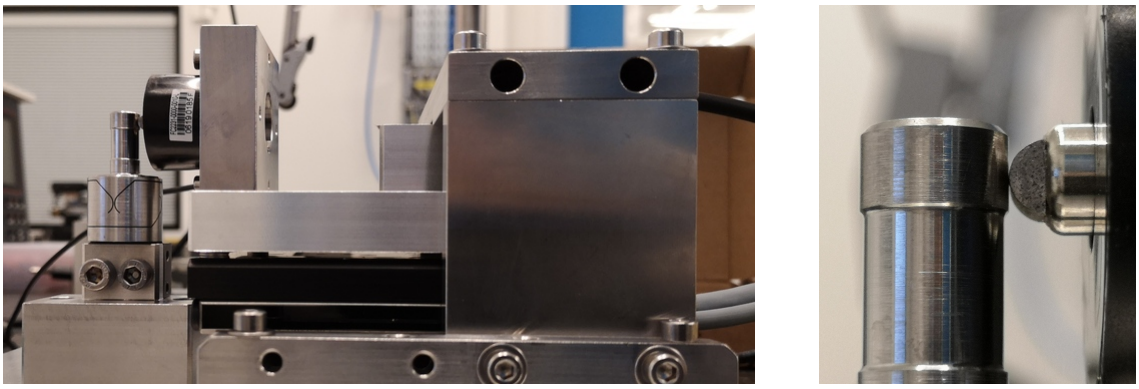

(a) Picture of the measurement bench

(b) Zoom on the tip

Figure 3.1: Manufactured test bench for compliance measurement of the flexible joints

3.1 Load Cell Calibration

In order to estimate the measured errors of the load cell "FC2231", it is compared against another load cell[1]. The two load cells are measured simultaneously while they are pushed against each other (see Figure 3.2a). The contact between the two load cells is well defined as one has a spherical interface and the other has a flat surface.

The measured forces are compared in Figure 3.2b. The gain mismatch between the two load cells is approximately 4 % which is higher than that specified in the data sheets. However, the estimated non-linearity is bellow 0.2 % for forces between 1 N and 5 N.

3.2 Load Cell Stiffness

The objective of this measurement is to estimate the stiffness k_F of the force sensor. To do so, a stiff element (much stiffer than the estimated $k_F \approx 1\,N/\mu m$) is mounted in front of the force sensor, as shown in Figure 3.3a. Then, the force sensor is pushed against this stiff element while the force sensor and the encoder displacement are measured. The measured displacement as a function of the measured

[1] XFL212R-50N from TE Connectivity. The measurement range is 50 N. The specified accuracy is 1 % of the full range

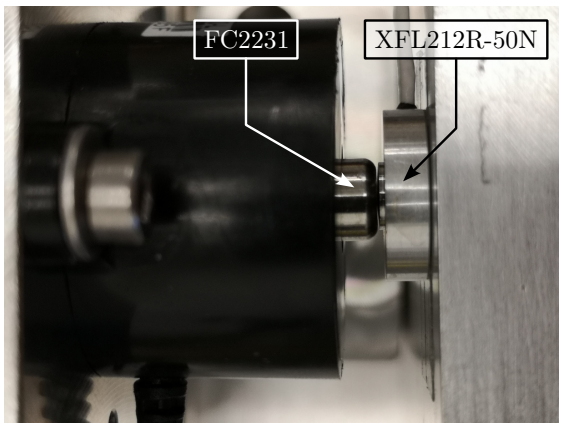

(a) Zoom on the two load cells in contact

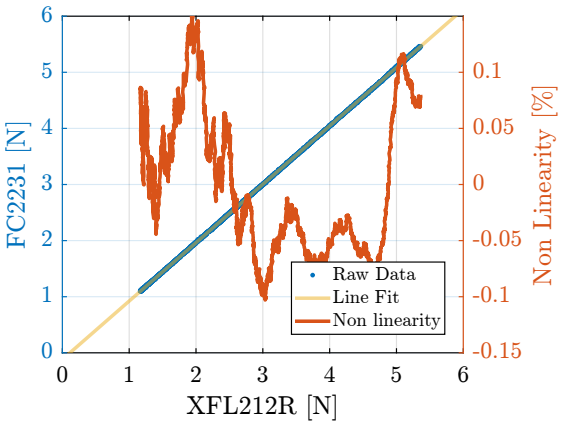

(b) Measured two forces

Figure 3.2: Estimation of the load cell accuracy by comparing the measured force of two load cells. A picture of the measurement bench is shown in (a). Comparison of the two measured forces and estimated non-linearity are shown in (b)

force is shown in Figure 3.3b. The load cell stiffness can then be estimated by computing a linear fit and is found to be $k_F \approx 0.68\,N/\mu m$.

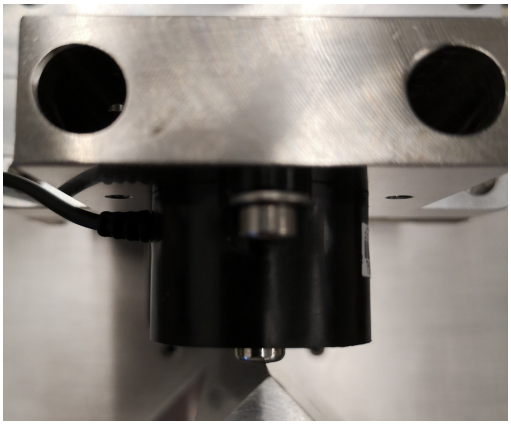

(a) Picture of the measurement bench

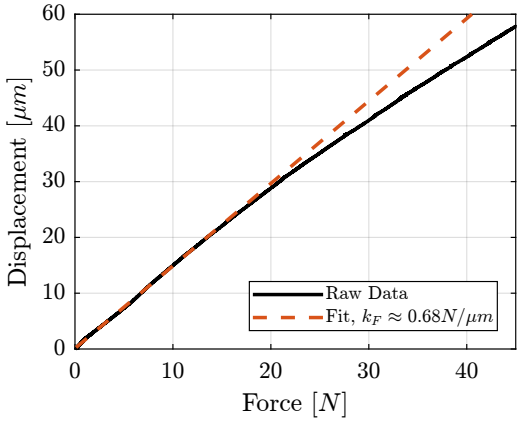

(b) Measured displacement as a function of the force

Figure 3.3: Estimation of the load cell stiffness. The measurement setup is shown in (a). The measurement results are shown in (b).

3.3 Bending Stiffness estimation

The actual stiffness is now estimated by manually moving the translation stage from a start position where the force sensor is not yet in contact with the flexible joint to a position where the flexible joint is on its mechanical stop.

The measured force and displacement as a function of time are shown in Figure 3.4a. Three regions can

be observed: first, the force sensor tip is not in contact with the flexible joint and the measured force is zero; then, the flexible joint deforms linearly; and finally, the flexible joint comes in contact with the mechanical stop.

The angular motion θ_y computed from the displacement d_x is displayed as function of the measured torque T_y in Figure 3.4b. The bending stiffness of the flexible joint can be estimated by computing the slope of the curve in the linear regime (red dashed line) and is found to be $k_{R_y} = 4.4\,Nm/\text{rad}$. The bending stroke can also be estimated as shown in Figure 3.4b and is found to be $\theta_{y,\max} = 20.9\,\text{mrad}$.

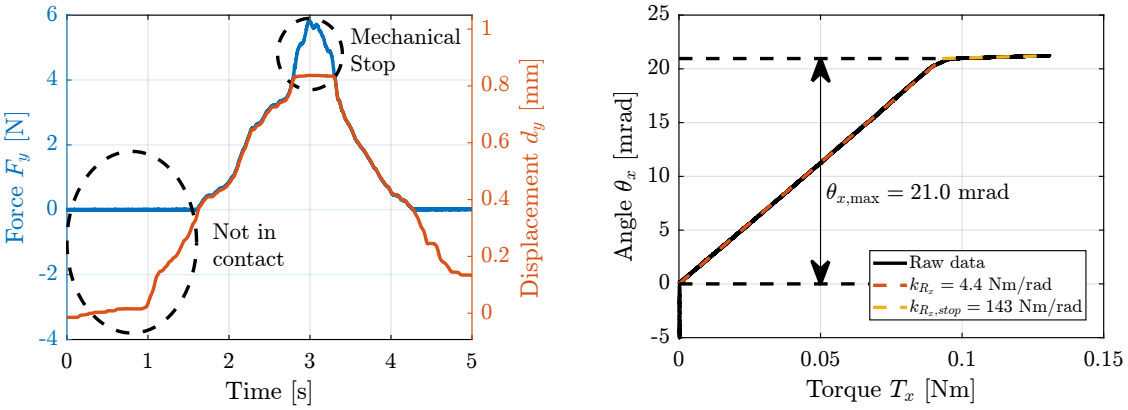

(a) Force and displacement measured as a function of time

(b) Angular displacement measured as a function of the applied torque

Figure 3.4: Results obtained on the first flexible joint. The measured force and displacement are shown in (a). The estimated angular displacement θ_x as a function of the estimated applied torque T_x is shown in (b). The bending stiffness k_{R_x} of the flexible joint can be estimated by computing a best linear fit (red dashed line).

3.4 Measured flexible joint stiffness

The same measurement was performed for all the 16 flexible joints, both in the x and y directions. The measured angular motion as a function of the applied torque is shown in Figure 3.5a for the 16 flexible joints. This gives a first idea of the dispersion of the measured bending stiffnesses (i.e. slope of the linear region) and of the angular stroke.

A histogram of the measured bending stiffnesses is shown in Figure 3.5b. Most of the bending stiffnesses are between $4.6\,Nm/rad$ and $5.0\,Nm/rad$.

Conclusion

The measured bending stiffness and bending stroke of the flexible joints are very close to the estimated one using a Finite Element Model ($k_{R_x} = k_{R_y} = 5\,Nm/\text{rad}$). The characteristics of the flexible joints are also quite close to each other. This should allow us to model them using unique parameters.

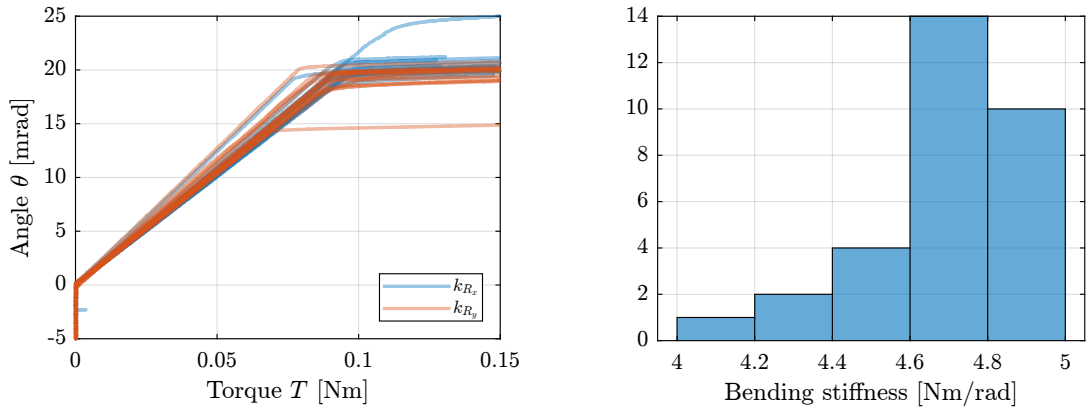

(a) Measured torque and angular motion for the flexible joints

(b) Histogram of the measured bending stiffness in the x and y directions

Figure 3.5: Result of measured k_{R_x} and k_{R_y} stiffnesses for the 16 flexible joints. Raw data are shown in (a). A histogram of the measured stiffnesses is shown in (b)

Conclusion

The flexible joints are a key element of the nano-hexapod. Careful dimensional measurements (Section 1) allowed for the early identification of faulty flexible joints. This was crucial in preventing potential complications that could have arisen from the installation of faulty joints on the nano-hexapod.

A dedicated test bench was developed to asses the bending stiffness of the flexible joints. Through meticulous error analysis and budgeting, a satisfactory level of measurement accuracy could be guaranteed. The measured bending stiffness values exhibited good agreement with the predictions from the finite element model These measurements are helpful for refining the model of the flexible joints, thereby enhancing the overall accuracy of the nano-hexapod model. Furthermore, the data obtained from these measurements have provided the necessary information to select the most suitable flexible joints for the nano-hexapod, ensuring optimal performance.